



Historical Sediment Source Apportionment in the Waimea Estuary

Continuation of the Waimea and Moutere River study

Prepared for Tasman District Council

December 2019

Prepared by:
Max Gibbs
Andrew Swales


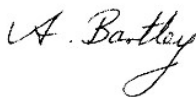

For any information regarding this report please contact:

Dr Andrew Swales
Water Quality Scientist
Freshwater Ecology
+64-7-856 1761
andrew.swales@niwa.co.nz

National Institute of Water & Atmospheric Research Ltd
PO Box 11115
Hamilton 3251

Phone +64 7 856 7026

NIWA CLIENT REPORT No: 2002012HN
Report date: December 2019
NIWA Project: TDC19201

Quality Assurance Statement		
	Reviewed by:	Sean Handley
	Formatting checked by:	Alison Bartley
	Approved for release by:	Michael Bruce

© All rights reserved. This publication may not be reproduced or copied in any form without the permission of the copyright owner(s). Such permission is only to be given in accordance with the terms of the client's contract with NIWA. This copyright extends to all forms of copying and any storage of material in any kind of information retrieval system.

Whilst NIWA has used all reasonable endeavours to ensure that the information contained in this document is accurate, NIWA does not give any express or implied warranty as to the completeness of the information contained herein, or that it will be suitable for any purpose(s) other than those specifically contemplated during the Project or agreed by NIWA and the Client.

Contents

Executive summary	5
1 Introduction	6
1.1 Objective.....	6
1.2 Background	6
2 Methods	9
2.1 Core Sampling.....	9
2.2 Core processing for dating.....	12
2.3 Core processing for stable isotope assessment.....	14
2.4 Source reference library samples	16
2.5 Additional information	17
2.6 Stop-banks, gravel extraction and high flow events.....	19
2.7 Selection of tracers for modelling using polygons.....	20
3 Results	21
3.1 Sediment accumulation rates.....	21
3.2 Stable isotopes and modelling.....	23
4 Discussion	26
4.1 Sediment accumulation rates (SAR)	26
4.2 CSSI analyses.....	28
5 Conclusions	30
6 Acknowledgements	32
7 References	33
Appendix A Study Proposal	35
Appendix B ESR Core dating results	38
Appendix C Isotopic data	41
Appendix D Floods in the Tasman District	42

Tables

Table 2-1: Site code descriptions for Figure 2-8.	17
Table 3-1: Core WA3 slice dates estimated from the lead-210 (210Pb) and 14C dating.	23

Table 3-2:	Summary of AMS radiocarbon dating results for cockle-shell valves sampled from a shell layer preserved in core WA-3 (96–99 cm depth), Waimea estuary.	23
------------	---	----

Figures

Figure 2-1:	Site photo for Waimea Estuary core Bell-Best Island site (WA3).	9
Figure 2-2:	Site map for Waimea Estuary Bell-Best Island site cores (WA3).	10
Figure 2-3:	Sediment accretion plate data from Waimea Estuary for 2018.	10
Figure 2-4:	Site photo for Moutere Estuary cores (Mo4).	11
Figure 2-5:	Screen shots of boat track and core site (Mo4).	11
Figure 2-6:	Site map for Moutere cores (Mo4).	12
Figure 2-7:	Waimea Estuary core WA3.	12
Figure 2-8:	Moutere Estuary core Mo4.	13
Figure 2-9:	Site map of source soil locations collected 16 December 2016.	17
Figure 2-10:	Production forest land clearance and development for cropping, pastoral farming and urban land use in the catchment adjacent to the Waimea Estuary.	18
Figure 2-11:	Common sources of sediment associated with soil erosion in the Waimea River catchment, not related to forestry.	18
Figure 2-12:	Soil library sample sites.	19
Figure 2-13:	Weekly maximum flows in the Waimea River since 1958.	20
Figure 3-1:	Core Mo4 (Moutere) - ages of sediment layers and lead-210 sediment accumulation rate (SAR) and sediment properties,	21
Figure 3-2:	Core WA3 (Waimea) - ages of sediment layers and sediment accumulation rates (SAR), and sediment properties.	22
Figure 3-3:	Examples using point-in-polygon testing for selecting suitable fatty acid isotopic tracer for isotopic modelling.	24
Figure 3-4:	Proportional contributions of soil sources from A) Subsoil, B) BankAg, C) PineR and D) PineH (see Table 2-1) in each depth slice from core WA3.	25
Figure 3-5:	Proportional contributions of soil sources from A) PineM, B) Native, C) pasture and D) G_&_B (see Table 2 1) in each depth slice from core WA3..	25
Figure 3-6:	Stacked bar graph of soil proportion results (0-100%) from the MixSIAR modelling.	26
Figure 4-1:	Data supporting the concept that the Best-Bell Island causeway may be producing a sediment trap effect at the monitoring site.	27
Figure 4-2:	High flow (>500 m ³ s ⁻¹) compared with the slice depths from core WA3 (yellow bars) from 1970 to 2018.	29

Executive summary

This report is a follow on from an earlier study by the National Institute of Water and Atmospheric Research Ltd (NIWA) for Tasman District Council (TDC), assessing the sources of sediment in the Waimea and Moutere Rivers by land use. In this study, the objectives were to determine 1) the sediment accumulation rates (SAR) in the Moutere and Waimea Inlets and 2) how land use soil source proportions have changed in recent years, using sediment cores from each inlet.

Difficulties with coring in Moutere Inlet resulted in high uncertainty for the lead-210 (^{210}Pb) dating, although an estimate of about 10 mm/yr ($r^2 = 0.224$) was obtained from the ^{210}Pb profile and ^{14}C data. Because of the lack of accurate ^{210}Pb dating, the Moutere core was not processed for soil source contributions.

In contrast, good cores were obtained from the Waimea Inlet at the Bell-Best Island site, which is used by TDC for sedimentation plate measurements. Using the ^{210}Pb dating technique, the SAR at this site was estimated at 7.2 mm/yr ($r^2 = 0.74$), which is comparable with the TDC SAR estimate at 8.00 mm/yr. The Bell-Best Island site is likely affected by the causeway between Bell and Best islands, constructed in 1981-1985, as the SAR at this site is >3 times higher than at any of the other sediment plate sites monitored by TDC.

Historical (pre-European) SAR value estimates obtained using ^{14}C data were in the range of 0.5-0.7 mm/yr.

Soil source contributions to the sediment in the Waimea Inlet were mainly from subsoil, agricultural erosion and harvested pine. Pasture (sheep), native forest and gorse and broom were also present but in minor proportions. Changes in source soil proportions over time were apparent, with past high flow (flood) events correlating with timing of catchment discharge and deposition of subsoils at specific dates recorded in NIWA's "NZ Historical Weather Events Catalogue", and most Council high flow data. While core slice subsoil proportions correlated with some high and low flow events, the lack of correlation at around 1980 (low flow but high subsoil contribution) could only be explained by river bed disturbance from gravel extraction and the start of the causeway construction from Best to Bell Island.

The compound specific stable isotope (CSSI) soil tracing results also indicated a reduction in the proportion of harvested pine soil runoff in the sediment versus an increase in agricultural soil runoff in recent years. This may be the result of canopy closure in the replanted pine forests and/or a change in agriculture practices and weather patterns in the catchment.

1 Introduction

Tasman District Council (TDC) has commissioned National Institute of Water and Atmospheric Research Ltd (NIWA) to undertake a study to determine the rate of sediment accumulation in the Waimea and Moutere Estuaries and the proportional changes in soil source contributions over time. This work follows on from the Waimea and Moutere River study (Gibbs and Woodward 2018), which was completed by NIWA in 2018, and is required to get as much information as possible about contemporary sedimentation rates and sediment source contributions to these estuaries.

The scope of the study was specified as follows:

- NIWA will undertake sediment core sampling as per the study proposal dated 24 May 2018 (See Appendix A) and as illustrated in the methods.
- NIWA will- collect cores from the two sites mentioned in our proposal dated 24 May 2018 (the blue zone in the Waimea estuary (Figure 2-1) and the green zone in Moutere estuary (Figure 2-4) and section them into between 12 and 15 slices each, i.e., 24 to 30 slices total.
- NIWA will perform core dating and compound specific stable isotope (CSSI) modelling calculations and produce a basic data report with minimal interpretation.
- NIWA will use the soil library from the previous river study for the modelling of the CSSI data.

1.1 Objective

The Gibbs and Woodward (2018) study set out the objective for this work, which was to identify and apportion the contemporary sources of sediment accumulating in the Waimea and Moutere estuaries by sub-catchment and then by land use. That study identified and apportioned the sources of soil, by sub-catchment, contributing to the sediment discharged from the Waimea and Moutere Rivers into their respective estuaries. This study apportions the source soils in the estuary sediments by land use and investigates the changes in sediment sources over time for recent (i.e., post 1970s) sediments.

1.2 Background

The Gibbs and Woodward (2018) study also gave the background for this work, as follows:

The Waimea and Moutere estuaries are highly valued environments for their aesthetics, biodiversity and uses for fishing, shellfish gathering and boating activities. Waimea Inlet in particular is regarded as a site of international importance for wading birds. The Lee, Roding and Wairoa catchments are some of the most heavily used rivers for recreational swimming in New Zealand. Therefore, these areas can be viewed as strategic assets for cultural and social wellbeing. Because of this importance, TDC has developed the Waimea Inlet Strategy which aims to create a sustainable future for these estuaries. The strategy brings together the communities of Tasman and Nelson and the many groups who have an interest in, and a commitment to, the Waimea Inlet in order improve the management of these areas.

Excessive fine sediment adversely affects rivers, estuaries and the coast. It affects rivers by smothering habitat within the bed that would otherwise be home to many invertebrates and fish (Thrush et al. 2004). Deposition of sediment sourced from erosion in the catchment of the Waimea and Moutere Rivers is a major problem in the Waimea and Moutere estuaries (Stevens and Robertson 2010, 2011 and 2014). Fine sediment reduces water clarity, interferes with feeding of filter feeding bivalves and crustacea and may smother benthic communities changing the biodiversity within the estuary (Norrko et al. 2002; Thrush et al. 2003a, 2003b). To reduce these inputs of sediment it is first necessary to understand what the sources of sediment are within the catchment so that management can be targeted. The information from this study will feed directly into this process and enable Council to develop a robust strategy for the management of the estuary and its catchment. The information will also be used for policy as directed by the NPS-FM.

While the national scale sediment load model of Hicks et al. (2011) predicts the long-term average sediment load per New Zealand rivers, based on fundamental characteristics of catchments (excluding land use per se), it does not account for shorter term variations within and between sub-catchments. These changes may be due to cyclical events such as harvesting, cultivation and planting activities. Sediment from flood events are included in the estimation of the annual average sediment load. The CSSI technique provides a means of evaluating contemporary differences in loads from sub-catchments and by land use source type from the contemporary source soil proportions in the deposited sediment at different locations down the river channel, while flood events may be detected at different depths in sediment cores from the receiving estuary or coastal waters.

An example of the effect of land use change on sediment yield is provided from the Pakuratahi Land Use Study (Eyles and Fahey 2006), which included a comparison of sediment yield from paired forestry and pasture catchments over a 12-year period. The results indicated that the farmed catchment produced almost four times more suspended sediment than the catchment in mature forest. This suggests there will be low sediment export from undisturbed native forest and mature pine forest plantations. However, the Pakuratahi Land Use Study also found that during harvesting, sediment yields from the forested catchment were about three times more than the farmed catchment, and therefore up to 12 times higher than before harvesting.

The Mahurangi Harbour study (Gibbs 2006) estimated the sediment yield to be up to 20 times higher than before harvesting, but that was a special case where harvesting drag lines inadvertently crossed a stream. Elevated sediment yield from harvested forest was expected to reduce to pre-harvest levels over a period of 2 to 3 years after replanting, as canopy closure from the trees and their root systems, once more protect the soil from erosion by rainfall (Eyles and Fahey 2006). During this period the erosion will decrease as weeds, native plants and the replanted pines create canopy cover thus protecting the bare land. Therefore, weed species, such as gorse and broom, provide a distinctive fingerprint signature that can also be used to define the plantation forests' land use status.

A review of more recent studies by Quinn and Phillips (2016) indicate that forestry practices may have improved. They say "Forest sediment yields at harvesting time can increase 5 fold over preharvest levels declining to preharvest levels often within 2-3 years of replanting." Basher et al. (2011) also found that forest harvesting was an important influence at small catchment scale, producing a five-fold increase in storm event sediment yield in the adjacent Motueka River catchment.

Changes in the level of sediment production are also likely to occur during the clearance of native forest, during cultivation of cropping land and clearance of land for urban development.

The history of the Waimea River flood control scheme also suggests that flood stop banks around the lower Waimea River may also be a source of sediment to the estuary. The stop banks constructed in the early 1900s from local soil were wiped out by big floods. The last of these was replaced in 1970 with no further stop bank failure recorded since.

It is also important to note that, while sediment production from the land use in the catchments is likely to deposit in the estuaries, the rate of accumulation at any given location in the estuary will depend on a number of factors including tidal currents and the existence of 'back waters' that may have been created by the placement of stop-banks and causeways e.g., the Best Island to Bell Island causeway was constructed between 1981 and 1985, and creates a slow flow zone in that area. Consequently, sediment accumulation rates across the estuary may be highly variable (see Figure 2-3).

2 Methods

2.1 Core Sampling

Sediment cores were collected from the Waimea and Moutere estuaries on 16-17 July 2018 to determine sediment accumulation rates (SAR) and identify sediment sources using the Compound Specific Stable Isotope (CSSI) technique (Gibbs, 2008). Cores up to 1.5 m long were sampled from intertidal flats using a vibra-corer with Diving Services Ltd. (Nelson).

A set of three cores were collected from the Waimea Estuary (16 July 2018) at the Bell-Best Island site WA3 (location: NZTM 1613299.2N, 5429168.7E) within the blue zone indicated in Figure 2-1 and map (Figure 2-2). This core site is within an area where TDC maintain a sediment accretion plate for monitoring seasonal–annual sedimentation. The sediment at this site is predominantly composed of mud. The sampled cores were 148, 110 and 142 cm long. The surface sediments were compact soft sediments, and the lower base of the cores was compact sand. The SAR at this site is likely influenced by the construction of the Best to Bell Island causeway between 1981 and 1985. This may be acting as a sediment trap as the Best-Bell Island site has the highest accretion rate of any of the TDC sites (Figure 2-3).

A set of three cores were collected from Moutere Estuary (17 July 2018) at site Mo4 (location: NZTM 1601716.0N, 5444739.6E). Initial trial cores and probing found unsuitable hard sediment within the green zone in Figure 2-4. Exploration further to the north found a zone containing soft mud of varying thickness, and a more suitable coring site (Figure 2-1, orange zone). The exact location of the core site is shown as screen shots of the boat track overlay (Figure 2-5) and map (Figure 2-6). The three cores were 90-95 cm long. The sediment was compact mud, with some sand and shells (cockles).



Figure 2-1: Site photo for Waimea Estuary core Bell-Best Island site (WA3). Blue zone has a mainly fine material. The alternative orange zone had courser material and was not sampled. The Best-to-Bell Island causeway is immediately downstream of the blue zone. [Photo provided by Trevor James, TDC].



Figure 2-2: Site map for Waimea Estuary Bell-Best Island site cores (WA3). Red square is the core site.

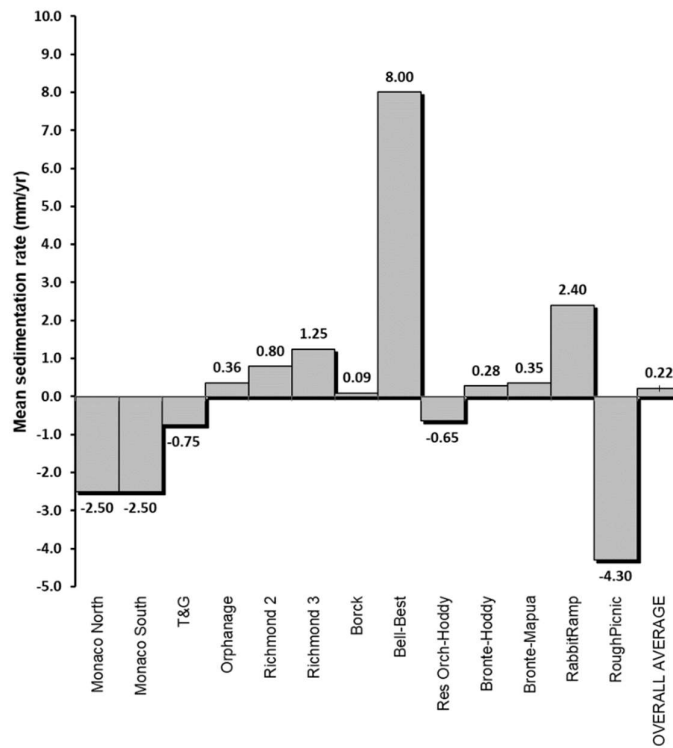


Figure 2-3: Sediment accretion plate data from Waimea Estuary for 2018. [Data from TDC].



Figure 2-4: Site photo for Moutere Estuary cores (Mo4). Green zone had compact sediment. The orange zone had fine muddy-sand material. The alternative purple zone had large gravel members beneath the mud and was not sampled. [Photo provided by Sean Handley, NIWA].

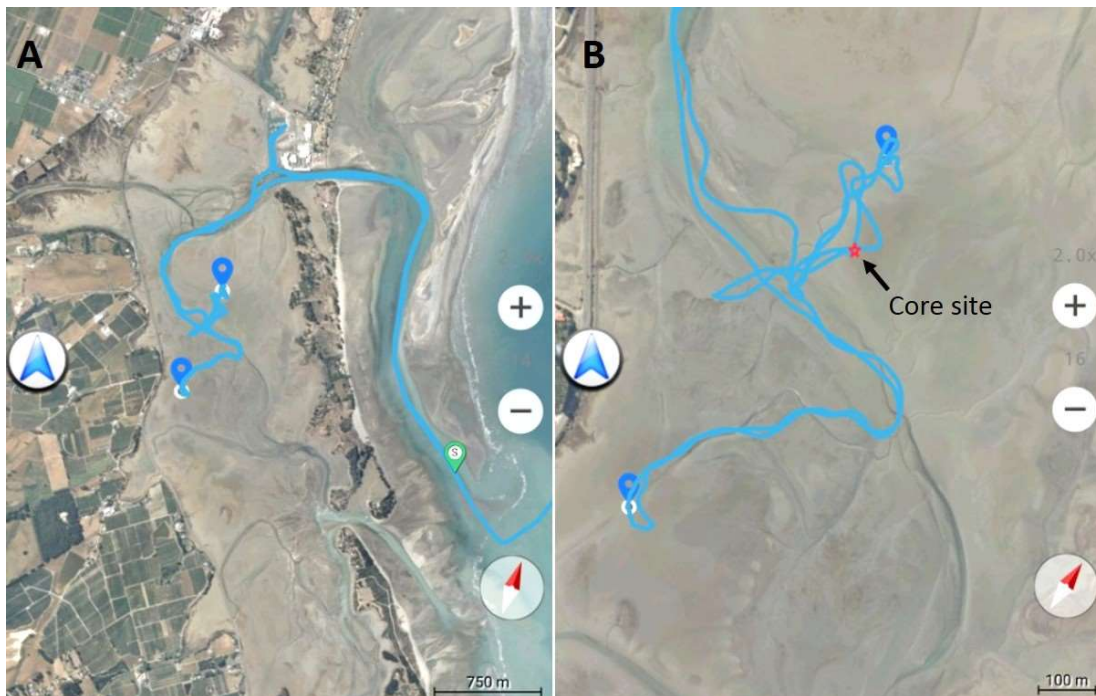


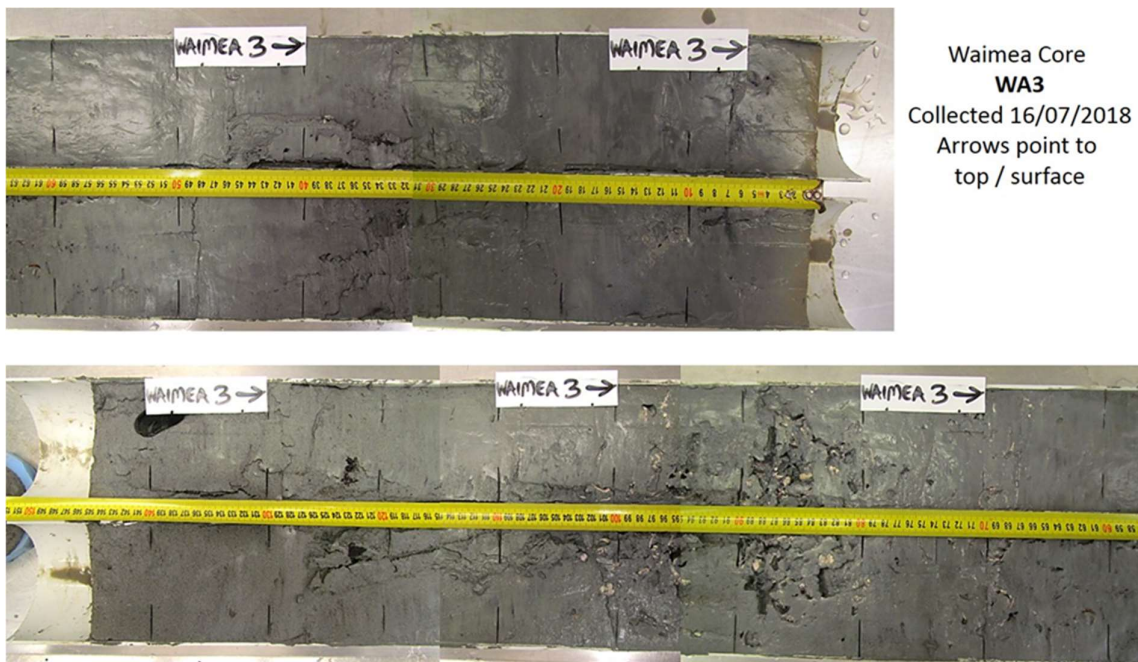
Figure 2-5: Screen shots of boat track and core site (Mo4). A) Shows a wide view of the estuary and boat track while searching for suitable sediment depth; B) focusses in on where the cores were taken. [Photos by Sean Handley, NIWA].



Figure 2-6: Site map for Moutere cores (Mo4). Red squares indicate the core sites.

2.2 Core processing for dating

The two cores, WA3 (Figure 2-7) and Mo4 (Figure 2-8), were split lengthwise for x-ray imaging and subsampling of 1-cm thick slices downcore for radioisotope analysis. Both cores showed the presence of shell beds at different depths, overlain with fine sediments.



Waimea Core
WA3
 Collected 16/07/2018
 Arrows point to
 top / surface

Figure 2-7: Waimea Estuary core WA3.



Figure 2-8: Moutere Estuary core Mo4.

2.2.1 Radioisotope dating

The sediment cores were processed in two stages to optimise the selection of samples for lead-210 (^{210}Pb) and caesium-137 (^{137}Cs) dating and estimation of time-averaged SAR. Samples at 5 to 10-cm increments down to 30–40 cm depth were initially analysed:

Moutere core Mo4: depth increments of 0–1, 4–5, 7–8, 10–11, 14–15, 17–18, 20–21, 24–25 and 29–30 cm.

Waimea core WA3: depth increments of 0–1, 4–5, 6–7, 8–9, 10–11, 14–15, 2–21, 24–25, 26–27, 29–30, 34–35 and 39–40 cm.

The sediment slices were subsequently freeze dried, ground to a fine powder and submitted to the Institute of Environmental Science and Research Limited (ESR) for gamma spectrometric measurement of total ^{210}Pb , caesium-137 and radium-226 (^{226}Ra). The excess ^{210}Pb ($^{210}\text{Pb}_{\text{ex}}$) component of the total ^{210}Pb , which is used for sediment dating, was determined from the total ^{210}Pb and ^{226}Ra activities (becquerels per kilogram [Bq kg^{-1}], where 1 Bq = 1 disintegration per second).

The initial results for core Mo4 displayed a poor fit to the log-linear regression model ($r^2 = 0.22$, $n = 9$) for estimating SAR and resulting low confidence in the sediment geochronology. No further analysis of core Mo4 was undertaken. By contrast, the (stage one) log-linear regression fit for core WA3 (Waimea estuary) was good and an additional four samples were analysed to fill gaps in the dated profile. A total of 13 sample were analysed in core WA3. The ^{210}Pb dating was used to estimate SAR during the post-European period (maximum ~ 150 years or seven half-lives [$t_{1/2} = 22$ years]). Caesium-137, derived from atmospheric-nuclear weapons tests since the mid-1940s was used to validate the ^{210}Pb geochronology. Maximum ^{137}Cs deposition occurred in the Southern hemisphere during 1963–1964 and was first detected in New Zealand in 1953 (Matthews, 1989). The maximum depth of ^{137}Cs in sediment deposits is the usual basis for dating in New Zealand estuaries as ^{137}Cs is derived from eroded catchment soils as well as direct atmospheric deposition. Due to the low initial ^{137}Cs activities in the 1950s and subsequent radioactive decay since that time (i.e., ~ 2 half lives, [$t_{1/2} = 30$ years]), the maximum ^{137}Cs depth will date to sometime during 1952–1963, and more likely towards the end of this period.

Sediment dating using two or more independent methods offsets the limitations of any one approach. This is important when interpreting sediment profiles from estuaries because of the potential confounding effects of sediment mixing by physical and biological processes (Smith, 2001). Sediment mixing by physical and biological processes in the surface mixed layer (SML) results in uniform radioisotope activities.

The ^{210}Pb dating also provide the basis for selecting sediment samples deposited during the post-European period for CSSI analyses of sediment sources by land use.

The split cores also revealed a dense layer of cockle-shell valves (*Austrovenus stutchburyi*) at 80–100-cm depth in the Waimea estuary core WA3 (Figure 2-7; Figure 2-8). Suspension feeding bivalves, including the New Zealand cockle are particularly suitable for radiocarbon dating as ^{14}C concentrations in cockles are similar to those found in shellfish previously used in accounting for marine reservoir effects (Hogg et al. 1998) using the marine ^{14}C calibration curve (Petchy et al. 2008).

Within this layer, three shell valves from different animals were selected (96–99-cm depth) for Accelerator Mass Spectrometry (AMS) ^{14}C (Radiocarbon) dating at the University of Waikato Radiocarbon Dating Laboratory. The AMS ^{14}C dating yields a conventional radiocarbon age (i.e., years before present, 1950 AD) to which a (^{14}C) marine-reservoir correction calibration curve is applied. This calibration step provides 95% probability calibrated dates for the sample age that are used to estimate time-averaged SAR. This analysis provided three independent ages for the cockle-shell layer from which a background/pre-human SAR could be estimated for comparison with the more recent post-European period.

2.2.2 Sediment properties

Physical properties of the Waimea estuary core WA3 were determined to identify changes in the composition of sediments that have accumulated at the site over time. The properties considered were sediment fabric, dry bulk density and particle size.

Particle size distributions (PSD, 0.1–300, 10–2000 μm) of sediment-core samples were determined using an Eye-Tech stream-scanning laser system, employing the time-of-transition (TOT) method to measure the diameters of individual particles (e.g., Jantschick et al. 1992).

Dry-bulk sediment density (ρ_b) profiles were determined for each core. The ρ_b was calculated as the dry mass per unit volume of sediment in each 1-cm thick core slice prepared for radioisotope dating. The slice volume was 78 cm^3 for the 10-cm diameter cores. Samples were processed by first weighing on a chemical balance to the nearest 0.01 g, dried at 70°C for 24 hours and reweighed to obtain the dry-sample weight. The ρ_b is expressed in units of grams per cubic centimetre (g cm^{-3}) and was calculated from the dry sample weight and sample volume. The ρ_b reflects the bulk characteristics of the sediment deposit, in particular sediment porosity (i.e., proportion of pore-space volume) and particle characteristics, such as size distribution and mineralogy. For example, the ρ_b of an estuarine sand deposit is of the order of 1.5–1.7 g cm^{-3} , whereas a mud deposit with high water content can typically have a ρ_b of $\sim 0.5 \text{ g cm}^{-3}$.

We note that the basal sediments are sands (1 to 1.4 m depth) and these transition to muds with a cockle bed at $\sim 0.7 - 0.9$ m depth.

2.3 Core processing for stable isotope assessment

Based on the ^{210}Pb dating results, core WA3 was sectioned into 15 slices to a depth of 34 cm with individual slices taken at selected depths: 1-2 cm, 5-6, 7-8, 9-10, 11-12, 13-14, 16-17, 18-19, 21-22, 23-24, 25-26, 27-28, 30-31, 32-33, 33-34 cm. The sediment slices were freeze dried and passed through a 500-micron (μm) mesh stainless steel sieve before sealing in a zip-lock type plastic bag pending stable isotope analysis.

2.3.1 Bulk isotope analysis

The proportion of organic matter in each sample was determined as loss on ignition (LOI) by combusting ~5 g aliquot of dried soil at 500 °C for three hours. Total organic carbon was estimated by multiplying the LOI result by 0.47 (Péridé and Ouimet 2008). Prior to carbon isotopic analyses, an aliquot of each sediment sample was acidified using 10% HCl to remove inorganic carbonates. Non-acidified samples were used for $\delta^{15}\text{N}$ analyses. Stable isotope analyses were carried out on a Delta V Plus continuous flow isotope ratio mass spectrometer (CF-IRMS) linked to a Flash 2000 elemental analyser using a MAS 200 R autosampler (Thermo-Fisher Scientific, Bremen, Germany) at the NIWA Environmental Stable Isotope Laboratory (Wellington, New Zealand). Isotope ratios are expressed in delta (δ) notation as $\delta^{13}\text{C}$ or $\delta^{15}\text{N}$ with units of per mil (‰). The carbon isotopic ratios were calibrated to a laboratory standard referenced to PeeDee belemnite carbonate and the nitrogen isotopic ratio was referenced to atmospheric nitrogen gas (N_2), respectively. Analytical working standards (DL Leucine or flour) were inserted on average every three samples. Standard deviations for the standards were $\pm 0.1\text{‰}$ for $\delta^{13}\text{C}$ and $\pm 0.2\text{‰}$ for $\delta^{15}\text{N}$. The stable isotope analyses also returned data on the %C and %N content of each sample.

2.3.2 Compound-specific stable isotope analyses (CSIA)

For compound specific stable isotope analysis (CSIA), a 20 g non-acidified aliquot of each sediment slice was extracted with dichloromethane (DCM) at 100°C at 2000 psi in a DIONEX ASE200 accelerated solvent extraction system, using two 5-minute extraction cycles, and combining the extracts. The bulk extract was rotary evaporated to dryness on a 35°C water bath. Free fatty acids (FA) were converted to FA methyl esters (FAMES) using 5% boron trifluoride (BF_3) catalyst in methanol heated to 70°C for 20 minutes in a sealed, screw-top reaction tubes. The resultant FAMES were extracted from the reaction mixture in hexane, dried and sent for analysed at the UC Davis, Stable Isotope Facility in California, USA.

Analysis was by GC-combustion-IRMS on an Agilent 6890 GC gas chromatograph (column: BP-5 (SGE), 30m, 0.25mm O.D., 0.25mm film; constant flow 1.4mL/min) coupled to Thermo MAT 253 through a GC-C-III combustion interface. Combustion was at 950°C with NiO/CuO catalyst and reduction at 650°C with Cu. The splitless injector was held at 280°C for 1 minute. The column temperature was held at 110°C for 1 minute before ramping to 220°C at 4°C/min then to 290°C at 10°C/min. The column was then held at 290°C for 10min. The methanol used in the methylation step was analysed for $\delta^{13}\text{C}$ by IRMS to allow correction of the FAME isotopic value for the added methyl group. A calibrated internal standard (C12:0 or C13:0) was added to each sample and reference mixture for use in both $\delta^{13}\text{C}$ and total C calculations. The average standard deviation of replicate measurements of reference materials was $< \pm 0.5\text{‰}$ across all FAMES. A methyl group correction was applied to all FAME data using the equation:

$$\delta^{13}\text{C}_{\text{FA}} = (\delta^{13}\text{C}_{\text{FAME}} - (1 - X) \delta^{13}\text{C}_{\text{Methanol}})/X \quad (1)$$

where $\delta^{13}\text{C}_{\text{Methanol}}$ is the bulk $\delta^{13}\text{C}$ value of the methanol used in the methylation process, $\delta^{13}\text{C}_{\text{FAME}}$ is the $\delta^{13}\text{C}$ value of the FA as measured, and X is the fractional contribution of the methyl group to the $\delta^{13}\text{C}$ of the FAME. The value X was calculated from the number of carbons in the FA molecule divided by the number of carbon atoms in the FAME derived from the FA. For example, the FA stearic acid (C18:0) has 18 carbon atoms whereas the FAME produced, methyl stearate, has 19 carbon atoms, including one added carbon from the methanol, and thus has an X value of 18/19 or 0.9474.

2.3.3 Seuss correction

Since the industrial revolution in the 1700s, the burning of fossil fuels has released CO₂ into the atmosphere with δ¹³C values reflecting the eon when coal and oil was created. This fossil CO₂ varies between fossil fuel sources (Andres et al. 1999) and is more isotopically depleted than the atmospheric δ¹³C-CO₂ values of present day. The admixing of the fossil CO₂ causes the isotopic δ¹³C values of the atmospheric CO₂ to become more depleted (Verburg 2007). Because plants use atmospheric CO₂ for growth, the CSSI values of the FAs in the plants will reflect the contemporary isotopic δ¹³C of the atmospheric CO₂. Consequently, the CSSI values of the FA biomarkers have been systematically changing since the mid-1700s and are presently about 2.2 ‰ more depleted than they would have been in 1700 AD. This is called the Seuss effect.

To use present day “contemporary” soil source library CSSI values to deconstruct the historical data in the sediment core slices, the convention is to make the CSSI values in each core slice more enriched by a Seuss correction value calculated for the time before present obtained from the dating.

As the Seuss effect only began around 1700 AD, all CSSI values from core sections before that time are made more isotopically enriched by 2.2‰, i.e., they are corrected by adding 2.2‰. Between 1700 AD and present-day values must be modified using an isotopic depletion number calculated from a 6th order polynomial equation and adding the absolute δ¹³C value (8.65‰) of present-day CO₂ (year 2018) as an offset to obtain the change in the δ¹³C isotopic value for the year (Y) of the core section (Verburg 2007).

$$\text{Correction value} = 8.65 + (7.7738118 \times 10^{-16} \times Y^6) - (1.2222044 \times 10^{-11} \times Y^5) + (7.1612441 \times 10^{-8} \times Y^4) - (2.1017147 \times 10^{-4} \times Y^3) + (3.3316112 \times 10^{-1} \times Y^2) - (273.715025 \times Y) + 91703.261 \quad (2)$$

2.4 Source reference library samples

Data from the 2016-17 study on the Waimea and Moutere Rivers (Gibbs and Woodward 2018) were used as the source reference library for deconstruction of the WA3 core. The source soils were selected to include native forest, pastoral sheep farming, bank erosion from agricultural land, newly harvested pine forest, older harvested pine runoff and subsoil from clearing forest land for agricultural and urban development. While the latter land clearance did not drain into the Waimea River, runoff from this type of land activity would likely reach the Waimea Estuary (Figure 2-9).

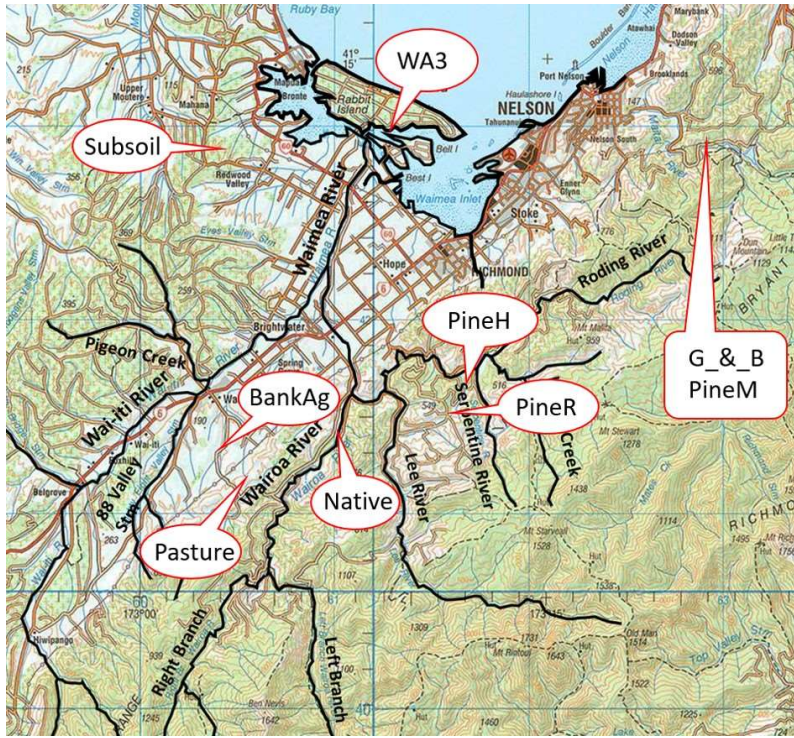


Figure 2-9: Site map of source soil locations collected 16 December 2016. From the Gibbs and Woodward (2018) report. Label points are approximate positions of the samples taken. See Table for all site descriptions.

Table 2-1: Site code descriptions for Figure 2-8.

Code	Sample description.
WA3	Waimea core site.
Subsoil	Subsoil after forest clearance and landscaping for agriculture and urban development.
BankAg	Bank erosion from agricultural land around Wakefield and Brightwater.
Pasture	Pasture for sheep farming. (Data averaged from several locations).
Native	Native forest above the Waioa River. (Data averaged from several locations).
PineM	Mature pine from Maitai River study (Gibbs and Woodward 2017).
PineH	Newly harvested pine but slash and understorey plants not disturbed (Kemp 2).
PineR	Older harvested pine sample taken from runoff in skidder pad area (Kemp 1).
G_&_B	Gorse and broom from Maitai River study (Gibbs and Woodward 2017).

2.5 Additional information

The **Subsoil** sample was collected from an area where production forest land had been cleared and was being developed for cropping, pastoral farming and urban land use in the catchment adjacent to the Waimea catchment (Figure 2-10). While runoff from this and other areas of similarly exposed subsoil (e.g., highway construction) do not drain into the Waimea River, sediment washed off this land in extreme weather events is likely to flow into the Waimea Estuary.



Figure 2-10: Production forest land clearance and development for cropping, pastoral farming and urban land use in the catchment adjacent to the Waimea Estuary. [From Gibbs and Woodward 2018].

The **BankAg** sample was collected near Richmond and represents non-pine forest sediment that comes from agricultural land. Bank erosion often occurs through undercut and collapse of stream banks or tracking where stock have access to the streams (Figure 2-11). This erosion also includes land slips, clearance of farm drains, having large areas of bare cultivated land on steep slopes, which can result in rilling even after the crops have been planted.

The **pasture** samples was from the base of steep sheep pasture along Pig Road (Figure 2-12F), and the **native** forest sample was collected where native forest came down to the Wairoa Gorge road (Figure 2-12E). The **PineM** sample represents mature pine (Figure 2-12A) and was a source collected for the Maitai River study (Gibbs and Woodward 2017). The **PineH** sample was from recently harvested pine above the Lee River where the slash and understory plants had not been removed and weed species were flourishing (Figure 2-12B). The **PineR** sample was collected from a skidder pad below harvested pine, where there was sediment runoff into the Lee River (Figure 2-12C). The **G_&_B** sample represents gorse and broom (Figure 2-12D) and was a source collected for the Maitai River study (Gibbs and Woodward 2017).

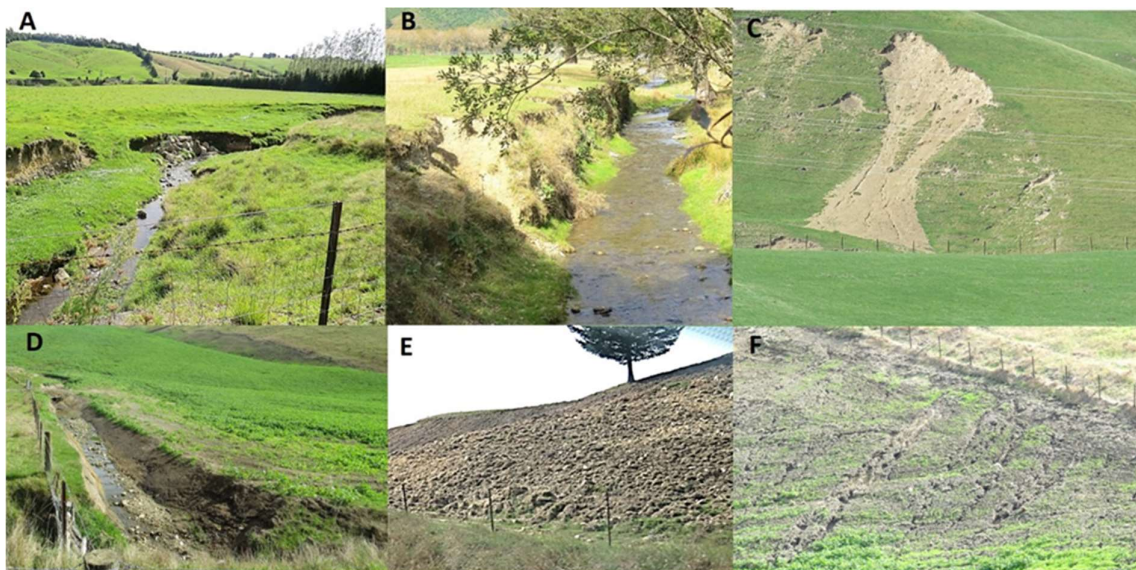


Figure 2-11: Common sources of sediment associated with soil erosion in the Waimea River catchment, not related to forestry. A) Stream bank collapse through undercutting; B) Stream bank erosion due to stock access; C) Earth flows and landslides on steep pasture; D) drain clearance leaving extensive bare soil exposed; E) Cultivation of steep hill sides leaving bare land vulnerable and exposed; F) Rilling of crop land on sloping land. [From Gibbs and Woodward 2018].

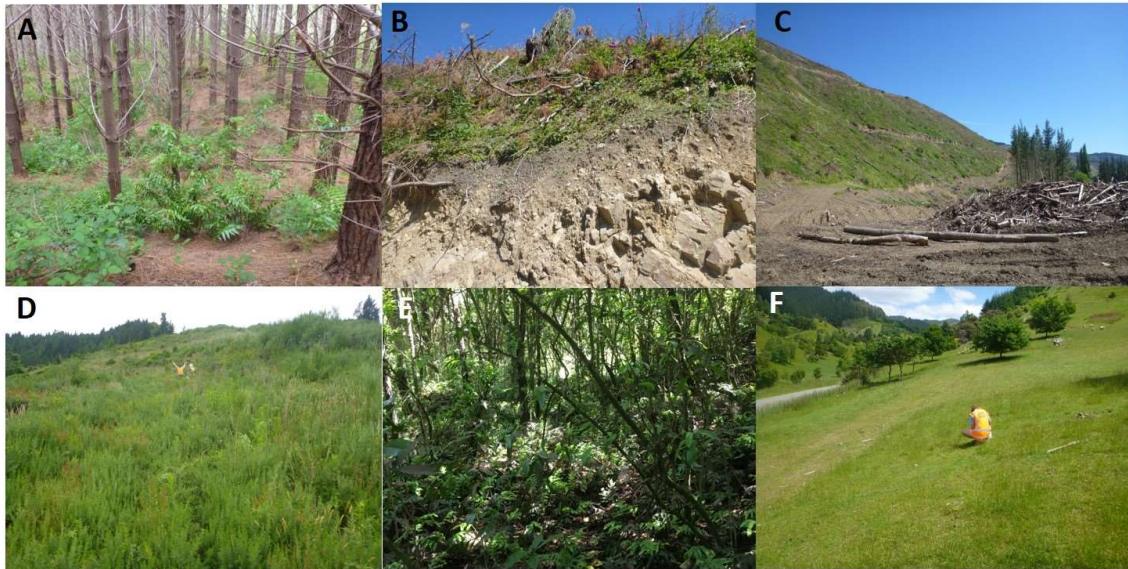


Figure 2-12: Soil library sample sites. A) **PineM** = mature pine; B) **PineH** = recently harvested pine forest without the removal slash and understory plants; C) **PineR** = harvested pine with disturbed soil running off into an adjacent stream; D) **G_&_B** = gorse and broom; E) **Native** = native forest; F) **Pasture** = sheep pasture on steep slopes.

2.6 Stop-banks, gravel extraction and high flow events

The stop-banks along the Waimea River were reconstructed in the 1950's with no further earthworks until a section downstream of Appleby Bridge was upgraded/raised in the late 1980's in response to effects from the 1983 flood (Giles Griffith, TDC, pers. Comm.). However, gravel extraction from the active riverbed in both the Waimea and Wai-iti Rivers was at its height up until the early 1980's, so this could have been a major source of fine sediment into the Waimea Estuary (Giles Griffith, TDC, pers. Comm.)

While there have been no massive floods since the stop banks were completed, there have been a number of high flow events, which have been loosely called 'floods', since that time. The TDC flow data shows that flow in the Waimea River is highly variable. Weekly flow maximum (maximum for the week) data range from 1 to 1732 $\text{m}^3 \text{s}^{-1}$ with an average weekly flow of 102 $\text{m}^3 \text{s}^{-1}$ in the 60-yr measurement period since 1958 (Figure 2-13).

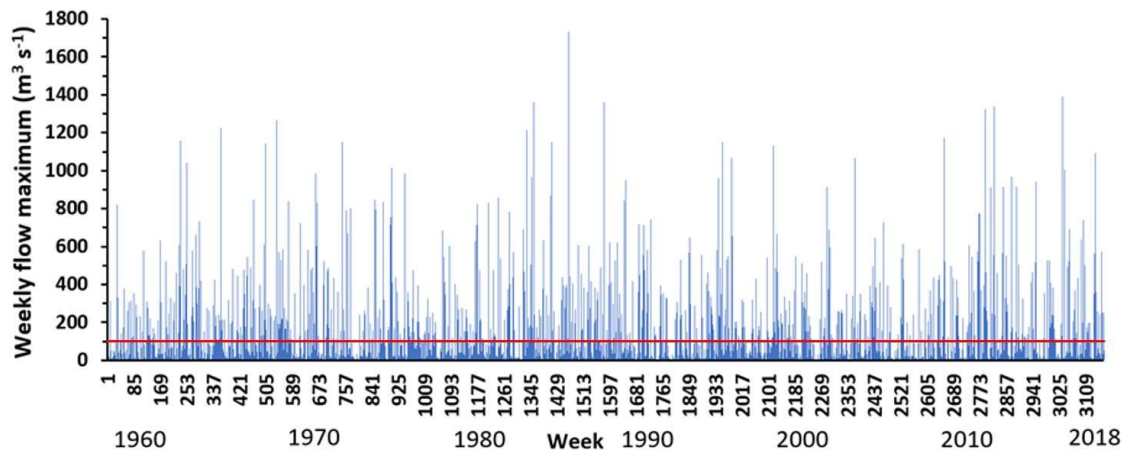


Figure 2-13: Weekly maximum flows in the Waimea River since 1958. Red line at $102 \text{ m}^3 \text{ s}^{-1}$ is the average flow over the 60-yr period of the graph. [TDC data].

2.7 Selection of tracers for modelling using polygons

Deconstruction of a sediment sample into its source component proportions used the mixing model MixSIAR (Stock et al. 2018). However, because mixing models are only as good as the data input, and the MixSIAR model will attempt to include all sources and tracers input from the reference library, it is essential to determine the most appropriate sources and sediment tracers from those sources before running the model. The recommended approach is to use an all-inclusive polygon test (Phillips et al. 2014), i.e., the sediment mixture isotopic data must lie within the bounds of a polygon drawn through the extreme values of the source isotopic data for biplots of pairs of isotopes, before these data can be used in the modelling. This criterion might not always be possible when assessing sediment cores using contemporary soil sources as there may have been sources present in the past that are no longer present.

2.7.1 Clarification of terms:

The sediment **mixture** is the core slice being deconstructed.

The **sources** are the land use material being tested against the mixture.

The **tracers** are the isotopic C and N signatures of the bulk soil and the $\delta^{13}\text{C}$ values of the FAs extracted from the mixture sediment and source soils. These include C14:0, C16:0, C18:0, C18:1, C18:2, C20:0, C22:0, C24:0 and C26:0.

2.7.2 Polygons for core WA3

A sequential step-wise approach testing the Seuss corrected mixture tracer data from the core sections against the same tracers from the eight selected contemporary sources determined that the most appropriate tracers were C16:0, C18:0, C20:0, C22:0 and C24:0. While the majority of the mixture tracers fall within the polygon, some are close to the polygon line connecting the source tracer values or just outside the line (e.g., Figure 3-3). Given that there was no sample replication for the core slices or the source samples, variability and possible missing historical source samples could account for this. With this in mind, these results are acceptable but will result in potentially larger error terms for those core slices close to the polygon lines.

3 Results

3.1 Sediment accumulation rates

The ^{210}Pb dating profile for the Moutere core Mo4 was not coherent with substantial scatter and no ^{137}Cs was detected. Consequently, the Moutere core could not be accurately dated and was not processed further on this occasion (Figure 3-1). The SAR for the Moutere core was estimated to be 10.0 mm/yr, $r^2 = 0.224$. In contrast, the ^{210}Pb dating profiles for the Waimea core WA3 was coherent and the ^{137}Cs line maximum occurred around 29-30 cm depth (Figure 3-2). The SAR for the Waimea core was estimated to be 7.2 mm/yr, $r^2 = 0.74$.

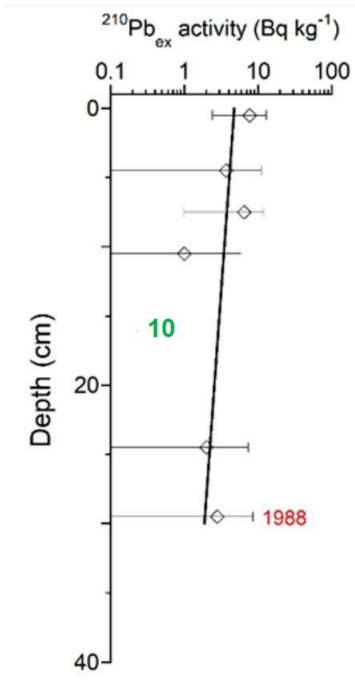


Figure 3-1: Core Mo4 (Moutere) - ages of sediment layers and lead-210 sediment accumulation rate (SAR) and sediment properties, Excess ^{210}Pb activity profiles with 95% confidence intervals shown. Radioisotope activity expressed in units of Becquerels (Bq kg^{-1}). Time-averaged SAR (Green text) was derived from regression fit to natural log-transformed ^{210}Pb data and ^{14}C ages of bivalve shells. Estimated ages of depth horizons (red text). Surface mixed layer (SML) to 4-cm depth inferred from excess ^{210}Pb profiles. Caesium-137 (^{137}Cs) data was inconclusive and could not be used to provide an accurate date for CSSI analysis.

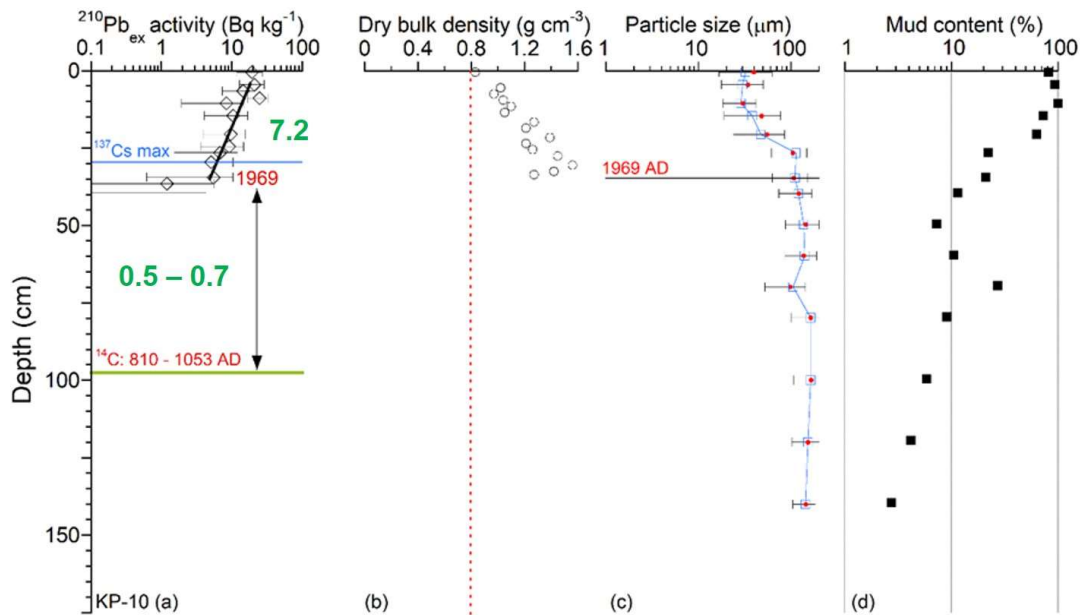


Figure 3-2: Core WA3 (Waimea) - ages of sediment layers and sediment accumulation rates (SAR), and sediment properties. (a) Excess ^{210}Pb activity profiles with 95% confidence intervals shown. Time-averaged SAR (Green text) derived from regression fit to natural log-transformed ^{210}Pb data and ^{14}C ages of bivalve shells. Estimated ages of depth horizons (red text). Surface mixed layer (SML) to 4-cm depth inferred from excess ^{210}Pb profiles. Maximum depth of caesium-137 (^{137}Cs) indicated. Radioisotope activity expressed in units of Becquerels (Bq kg^{-1}). (b) Sediment dry bulk density; (c) mean (red) and median particle diameters with standard deviation; and (d) mud content as percentage of sample by particle volume.

The best estimates of core depth dating for WA3 are presented in Table 3-2 and cover the recent sediments back to year 1971. These dates were used to apply the Seuss correction to the isotopic data for the CSSI analyses.

The longer-term dating extended back to about 1400 years before present (BP) (Table 3-2). These dates were determined from the AMS ^{14}C data radiocarbon dating results for cockle-shell valves sampled from a shell layer preserved in WA3 core at a depth of 96–99 cm in the Waimea estuary. This data gave a ^{14}C SAR (calibrated) age range of 0.5-0.7 mm/yr. This range is based on the average values of the 95% probability age ranges (lower and upper) for the 3 individual cockle shells.

Table 3-1: Core WA3 slice dates estimated from the lead-210 (210Pb) and 14C dating.

WA3 Core slice	year
1-2cm	2016
5-6cm	2010
7-8cm	2008
9-10cm	2005
11-12cm	2002
13-14cm	1999
16-17cm	1995
18-19cm	1992
21-22cm	1988
23-24cm	1985
25-26cm	1983
27-28cm	1980
30-31cm	1976
32-33cm	1973
33-34cm	1971

Table 3-2: Summary of AMS radiocarbon dating results for cockle-shell valves sampled from a shell layer preserved in core WA-3 (96–99 cm depth), Waimea estuary.

NIWA Sample ID	UoW Lab Wk number	Conventional Age (yr BP)	Calibrated Age - upper (yr BP)	Calibrated Age - lower (yr BP)
WA-3_97-98 cm	Wk-49375	1,465 ±18 BP	910	1,150
WA-3_96-98 cm	Wk-49374	1,415 ±19 BP	860	1,110
WA-3_97-98.5 cm	Wk-49187	1,478 ±15 BP	920	1,160

3.2 Stable isotopes and modelling

3.2.1 Biplots

Selected FA biomarker tracers used for modelling were plotted as bi plots. These bi-plots are the basis of the point-in-polygon tests for determining the suitability of different tracers for use in the modelling.

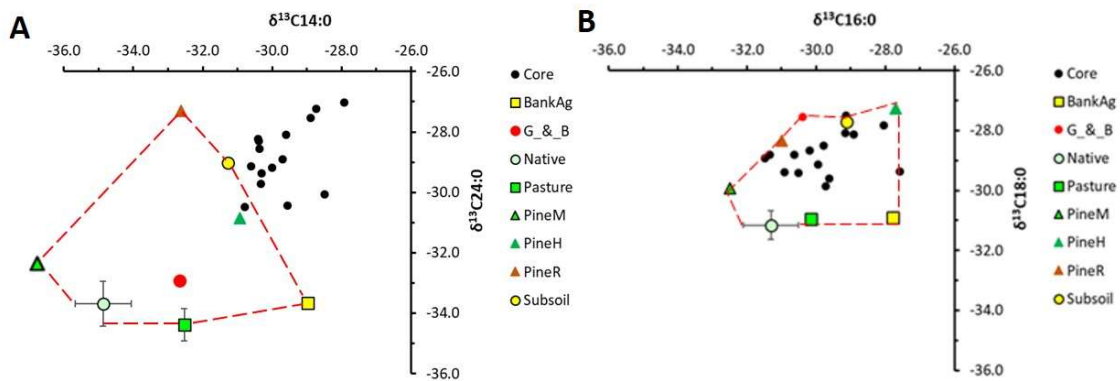


Figure 3-3: Examples using point-in-polygon testing for selecting suitable fatty acid isotopic tracer for isotopic modelling. Error bars on native and pasture sources are ± 1 standard deviation about the mean. All other sources were from single sites.

Bi-plots of tracer isotope pairs from source soils sampled from the Waimea River Catchment (Gibbs & Woodward 2018) were compared relative to the Seuss corrected core mixtures from the present study (Figure 3-3, black dots). Graph Figure 3-3A shows that the polygon (red dashed line) drawn through the source data for C14:0 and C24:0 tracers does not enclose all the core data points (black dots) meaning at least one of these tracers is not suitable for use in modelling. Conversely, graph Figure 3-3B shows that the sediment core data all lie within the bounds of the polygon and meet the requirements for a point-in-polygon assessment (Phillips et al., 2014) meaning that both of these tracers are suitable for modelling. From this point-in-polygon assessment, only the tracers C16:0, C18:0, C20:0, C22:0 and C24:0 were suitable for use in the modelling.

The complete isotopic data set for the tracers in core WA3 are presented in Appendix C together with the data for the nine sources used.

3.2.2 Source soil proportion profiles for core WA3

The isotopic data were converted to source soil proportions in the individual core slices from core WA3 using MixSIAR and are visualised as mean % soil relative to depth and estimated date in Figure 3-4 and Figure 3-5. As with all MixSIAR model outputs, the values are not absolute and represent the best estimates produced from the model using the selected tracers. As there were only single samples available for the source soils and the sediment mixtures, the error term is unknown.

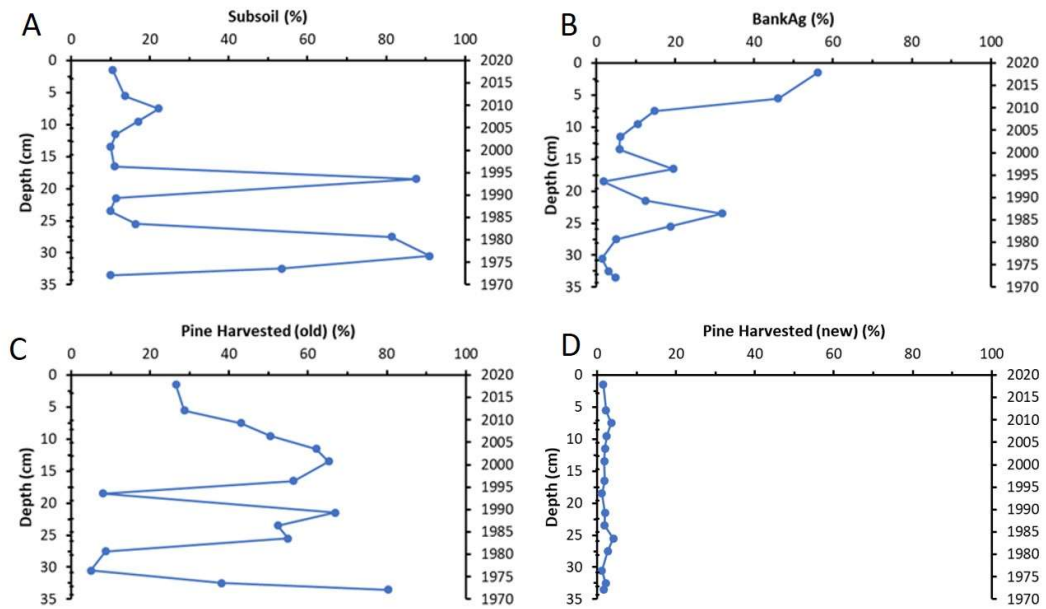


Figure 3-4: Proportional contributions of soil sources from A) Subsoil, B) BankAg, C) PineR and D) PineH (see Table 2-1) in each depth slice from core WA3. Soil contribution in % soil is compared with depth (left axis) and estimated date (right axis) for each source soil tested

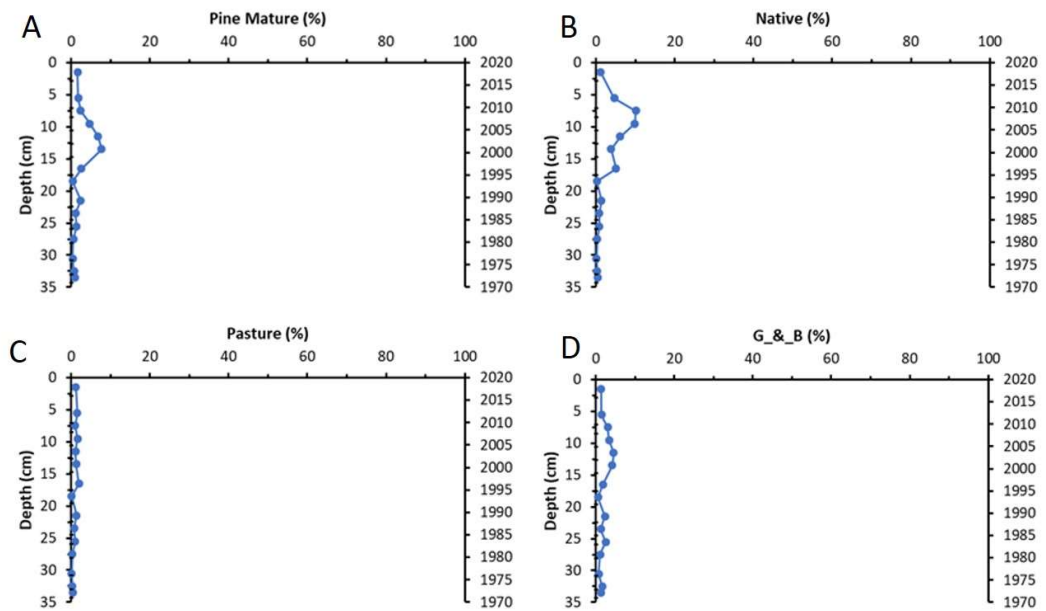


Figure 3-5: Proportional contributions of soil sources from A) PineM, B) Native, C) pasture and D) G_&_B (see Table 2 1) in each depth slice from core WA3.. Soil contribution in % soil is compared with depth (left axis) and estimated date (right axis) for each source soil tested

The soil proportions are presented as a stacked bar graph for each date step (Figure 3-6).

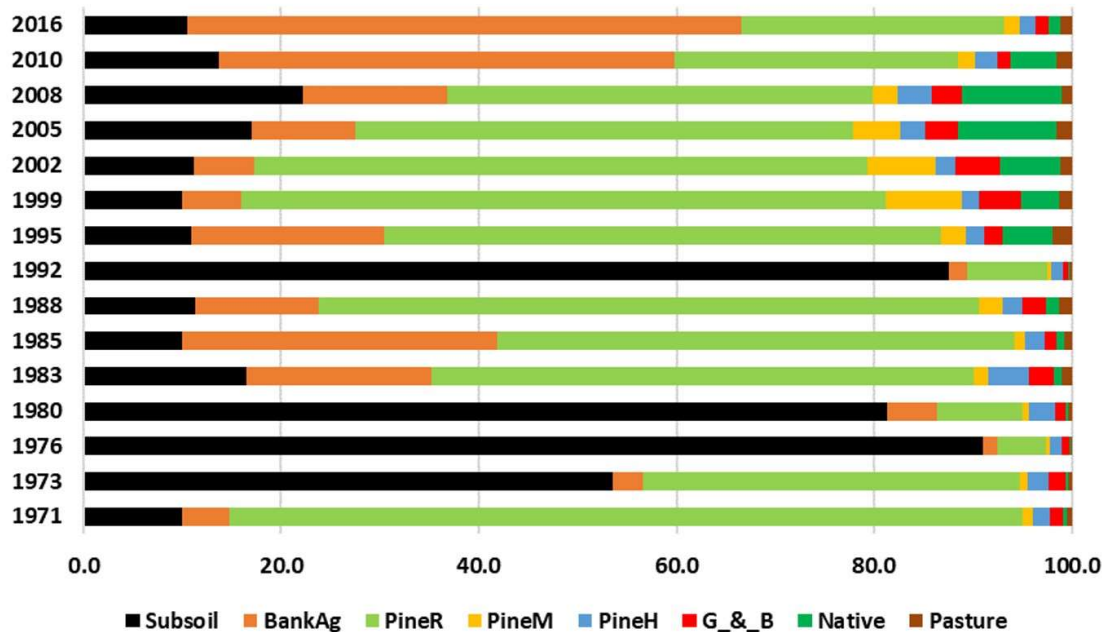


Figure 3-6: Stacked bar graph of soil proportion results (0-100%) from the MixSIAR modelling. Data are in order (left to right) from largest to smallest contributors.

4 Discussion

The main objective of the 2018 study was to identify and apportion the contemporary sources of sediment accumulating in the Waimea and Moutere estuaries by sub-catchment and then by land use. That study identified and apportioned the sources of soil, by sub-catchment, contributing to the sediment discharged from the Waimea and Moutere Rivers into their respective estuaries. The purpose of this study was to determine the sediment accumulation rates in the Waimea and Moutere estuaries and then determine and apportion the source soils contributing to the sediments in these estuaries by land use and investigates the changes in sediment sources over time for recent (i.e., post 1970s) sediments.

4.1 Sediment accumulation rates (SAR)

To determine SAR, sediment cores were taken from each estuary. There was considerable difficulty obtaining the cores from the Moutere estuary as the mud flats were very hard. After searching across various parts of the estuary (see boat track Figure 2-5), an apparently suitable soft mud site was found and a core, Mo4, was collected (Figure 2-8). Observations from the core showed a sharp demarcation between a deeper cockle bed and the overlying mud at around 20 cm depth (Figure 2-8). However, the radioisotope analysis results showed that there was large scatter in the ^{210}Pb data but no ^{137}Cs data (Figure 3-1). A best estimate for SAR obtained from the ^{210}Pb data and ^{14}C data from shell fragments was 10 mm/yr but with a relatively high level of uncertainty ($r^2 = 0.224$).

The reason for the lack of structure in the ^{210}Pb data and the lack of ^{137}Cs data implies mixing with sufficient energy to ablate the harder surface of the mudflats and resuspending the finer surficial sediments. A possible source of this mixing energy could be tidal, with strong currents across the mud flat as the water flows in and out around both ends of Jackett Island to get into and out of the Moutere Inlet. These currents could be exacerbated by wind waves as the Moutere Inlet is an

elongated open body of water (around high tide) aligned with the prevailing west-to-southwest winds.

In contrast with the Moutere sediment core, the sediment core from the Waimea Inlet (WA3) was easier to obtain and had a coherent pattern consistent with isotopic decay ^{210}Pb . The core also had a measurable ^{137}Cs signature with a maximum at a depth of about 30 cm (Figure 3-2A). The best estimate of SAR for the Waimea core was 7.2 mm/yr with a higher level of certainty ($r^2 = 0.74$).

The WA3 site was located at the Bell-Best site used by TDC to estimate SAR with sediment accretion plates. The TDC SAR data for this site in 2018 was 8.00 mm/yr (Figure 2-3). The SAR estimate from this study using radionuclide dating, although not the same, is comparable with the accretion plate data. The difference is likely due to natural interannual variability, with the SAR estimate from this study being an integrated average over about 40 years since 1980 while the TDC estimate was for the year 2018.

It is apparent, from the TDC SAR data (Figure 2-3), that sediment accumulation is highly variable across the Waimea Estuary. That the SAR is highest at the Bell-Best Island monitoring site suggests that this site is a sediment sink. TDC suggested that the construction of the causeway from Best Island to Bell Island in 1981 to 1985 may have influenced the sediment accumulation at this site, possibly providing a sediment trap effect. A closer look at the sediment from the core around 1980 to 1990 (Figure 4-1A) shows a colour change to darker sediment since 1985. This date also coincides with a marked reduction in particle size and an increase in the proportion of mud at this site (Figure 4-1B). Together these data support the concept of the causeway having a sediment trap effect (Figure 4-1).

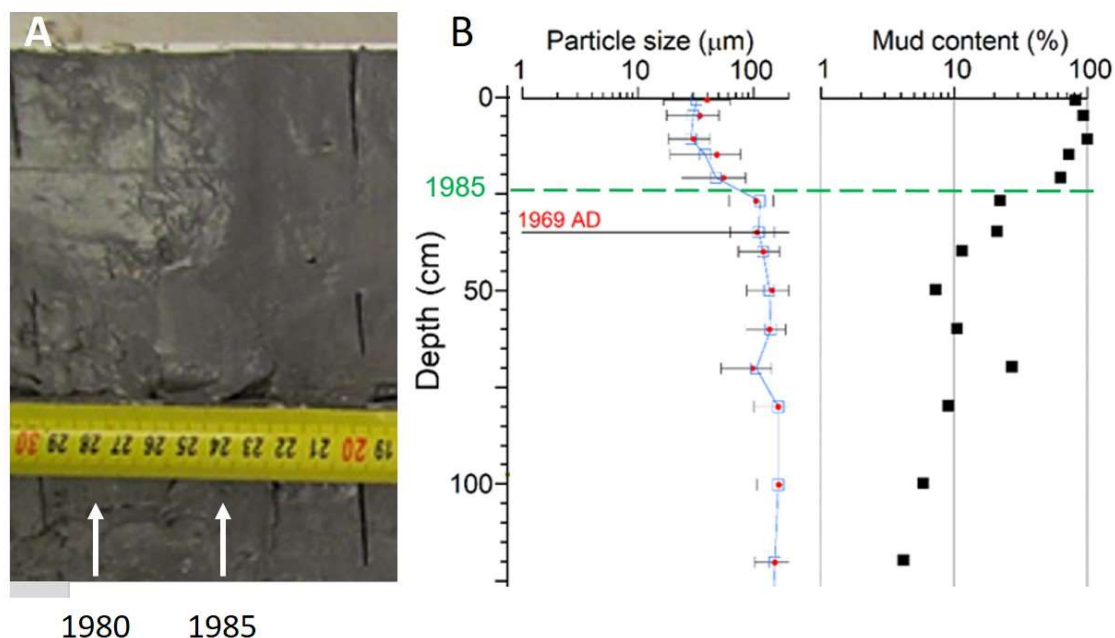


Figure 4-1: Data supporting the concept that the Best-Bell Island causeway may be producing a sediment trap effect at the monitoring site. A) Sediment colour and texture changed at depth 24-cm, which is equivalent to year 1985 (from Figure 2-7), B) Particle size decreased and mud content increased markedly after year 1985 (extracted from Figure 3-2). Green dashed line represents year 1985 when the causeway was completed.

Historical SAR values as determined by AMS radionuclide ^{14}C data, gives a ^{14}C SAR (calibrated) age range of 0.5-0.7 mm/yr.

4.2 CSSI analyses

The isotopic signatures of the FAs extracted from the WA3 core slices showed acceptable patterns in the point-in-polygon biplots (Figure 3-3), although some core data points lay outside the polygon line for some tracers. The tracers C16:0, C18:0, C20:0, C22:0 and C24:0 were found to be suitable for modelling and were used. The isotopic signature profiles (data Appendix C) indicated vertical depth structure for some tracers and a general trend of increasing enrichment with depth. Profiles of the modelled data converted to source soil proportions showed strong differences down the depth of the core with the majority of the sediment coming from three main sources: subsoil, BankAg and Pine R (Figure 3-4). The remaining sources tested were present but only in low proportions (Figure 3-5).

When presented as a stacked bar graph (Figure 3-6), the results show several strong discrete layers where subsoil was the dominant source of the sediment. The most prominent of these was a layer at a depth of 18-19 cm representing a date of 1992. Because this layers' soil source proportions were very different from the soil source proportions before and after, it must represent an event at about that time – most likely a 'flood'. Data extracted from the NIWA "NZ Historical Weather Event Catalog" (Appendix D) shows one major flood event close to that time, in 1990, with no significant events from 1988 (cyclone Bola) before, to 1997 after. The 1990 record describes the event as follows:

- **August 1990 Tasman-Nelson Flooding and the Taranaki Tornado**
Severe damage to homes and businesses occurred when a tornado hit Bell Block and Inglewood on the 12th of August 1990. Tasman-Nelson experienced heavy rain causing extensive flooding in the Motueka area and resulting in millions of dollars' worth of damage. Marlborough also experienced some flooding.

With the date of the flood event recorded very precisely, this allows an assessment of the precision of the radionuclide dating technique. The core slices were 1-cm thick taken at 2-cm increments (Table 3-1). The 1992 slice was for a 1-cm thick slice from 18-19 cm. The next deeper slice was 1-cm thick from 21-22 cm and was dated as about 1988. The intermediate two 1-cm increments would have been 20-21 cm and 19-20 cm to cover the four years from 1988 to 1992. This suggests that the slice from 19-20 cm would likely be about 1990. This indicates very good agreement between the radioisotope dating and the historical records and gives confidence in the identified soil source proportions at other dates.

A point to consider, however, is that the precision of the source soil determination in the 1-cm thick slices raises the possibility that an event may have been missed where the gap between slice depths is large enough. To assess this possibility, the relationship between high flow/flood events and changes in sediment sources was checked. High flow events were selected from the weekly maximum flow data (Figure 2-13) arbitrarily limited to flows >5 times the 60-yr average (Figure 4-2) to reduce the "noise" in the data. The core slice sample increments were overlaid to determine how these aligned with high flows and events indicated by subsoil erosion component in the stacked graph (Figure 3-6).

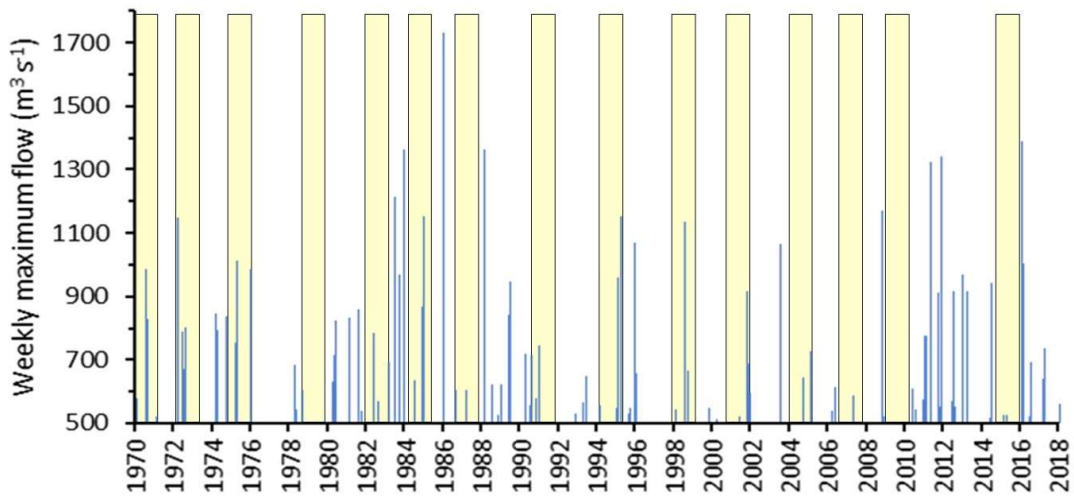


Figure 4-2: High flow (>500 m³ s⁻¹) compared with the slice depths from core WA3 (yellow bars) from 1970 to 2018.

It is apparent from Figure 4-2 that the core slices have caught the trailing edge of the 1990 high flow event as well as 1973 and 1976 events. The slices did not coincide with any high flow event in 1980, and yet the CSSI model results show a large proportion of subsoil at that time. Since the causeway was being constructed around that time and active riverbed gravel extraction in both the Waimea and Wai-iti Rivers was at its height up until the early 1980's (Giles Griffith, TDC, pers. Comm.), the subsoil sediment identified in the 1980 core slice could have come from river bed disturbance.

The 1983 flood event was missed completely and is not seen in the stacked graph data.

In more recent times to the present, the proportions of subsoil have remained relatively constant but the proportion of BankAg soil source have been increasing while the proportion of PineR soil source have been decreasing (Figure 3-6). This implies a change in the erodible soil sources in the catchment. This may reflect the growth of the juvenile pine forest, with replanting reaching a closed canopy state that reduces the erosion associated with the recently harvested pine (cf. Pakuratahi land use study: Eyles and Fahey, B. 2006). At the same time, agricultural practices and weather patterns may have changed with wetter spring weather coinciding with the cultivation of land for cropping.

5 Conclusions

- Sediment core dating in the Moutere Inlet had a level of inaccuracy because of the hard substrate affecting the ability to take sediment cores, most likely due to disturbance of the surficial sediment by tidal currents and wind waves in the shallow water.
- The sediment core site in the Waimea Inlet Best-Bell Island site was appropriate and provided good cores for radionuclide dating.
- Sediment accumulation rate (SAR) estimates suggest 10.0 mm/yr in the Moutere Inlet but with elevated level of uncertainty ($r^2 = 0.224$) because of the lack of good ^{210}Pb data and absence of ^{137}Cs data. Because of the lack of accurate ^{210}Pb dating, the Moutere core was not processed for soil source contributions.
- The SAR at the Waimea Inlet Best-Bell Island site was estimated at 7.2 mm/yr with a higher level of certainty ($r^2 = 0.74$). This estimate is comparable with the sedimentation rate of 8.00 mm/yr estimated at this site by TDC, using sediment accretion plates.
- The TDC sediment accretion plate SAR data from other sites in the Waimea Inlet were substantially lower than at the Best-Bell island sampling site suggesting that this site was being influenced by the causeway (installed between 1981-1985), which probably created a sediment trap effect.
- Sediment core texture changed, particle size decreased and mud content increased after 1985, supporting the concept of an influence from the causeway.
- Historical (pre-European) SAR value estimates obtained using ^{14}C data were in the range of 0.5-0.7 mm/yr.
- Soil source contributions to the sediment in the Waimea Inlet were mainly from subsoil, agricultural erosion and harvested pine. Pasture (sheep), native forest and gorse and broom were also present but in minor proportions, although the results showed some changes over time.
- These soil proportions changed over time and high flow events were apparent as sudden increases in the proportions of subsoil.
- There were very good correlations between the CSSI data for the 1990 flood event and recorded in the NIWA “NZ Historical Weather Event Catalogue”, as well as high flow events (TDC data) confirming the validity and precision of the radionuclide dating technique.
- There were also good correlations with earlier 1970s high flow events. However, a lack of correlation between high subsoil contributions and low flows around 1980 suggest that riverbed disturbance from gravel extraction and the earthworks for the Best to Bell Island causeway around that time may have been a sediment source.
- The CSSI results indicated a reduction in the proportion of harvested pine soil runoff in the sediment versus an increase in agricultural soil runoff in recent years. This may indicate that canopy closure for replanted pine forest was reducing runoff. It may also indicate a change in land use in some areas of the catchment or possibly effects of

wetter springs coinciding with soil cultivation leaving bare soil prepared for crop planting, exposed to heavy rain.

6 Acknowledgements

We thank Sean Handley (NIWA) for coordinating the collection of the sediment cores for this study.

7 References

- Andres, R.J., Fielding, D.J., Marland, G., Boden, T.A., Kumar, N., Kearney, A.T. (1999) Carbon dioxide emissions from fossil-fuel use, 1751–1950. *Tellus B*, 51: 759–765.
- Basher, L.R., Hicks, D.M., Clapp, C., Hewitt, T. (2011) Sediment yield response to large storm events and forest harvesting, Motueka River, New Zealand. *New Zealand Journal of Marine and Freshwater Research*, 45, 3: 333-356. DOI: 10.1080/00288330.2011.570350.
- Eyles, G., Fahey, B. (eds) (2006) Pakuratahi land use study. *Hawkes Bay Regional Council report HBRC plan number, 3861*. June: 128.
www.hbrc.govt.nz/Land/PakuratahiLandUseStudy/tabid/299/Default.aspx
- Gibbs, M., Woodward, B., (2017). CSSI-based sediment source tracking study for the Maitai River, Nelson. *NIWA Client Report* No: 2017256HN, prepared for Nelson City Council: 46.
- Gibbs, M. (2006a) Source Mapping in Mahurangi Harbour. *Auckland Regional Council Technical Publication*, TP321.
- Gibbs, M., Woodward, B. (2018). Waimea and Moutere Sediment Sources by Land Use. *NIWA Client Report* No: 2018026HN, prepared for Tasman District Council: 63.
- Hicks, D.M., Shankar, U., McKerchar, A.I., Basher, L., Lynn, I., Page, M., Jessen, M. (2011) Suspended Sediment Yields from New Zealand Rivers. *Journal of Hydrology (New Zealand)*, 50: 81-142.
- Hogg, A.G., Higham, T.F.G., Dahm, J. (1998) Radiocarbon dating of modern marine and estuarine shellfish. *Radiocarbon*, 40: 975–984.
- Matthews, K.M. (1989) Radioactive Fallout in the South Pacific – a History. Part 1. Deposition in New Zealand. *Report*, NRL 1989/2. National Radiation Laboratory: Christchurch.
- Norkko, A., Thrush, S.F., Hewitt, J.E., Cummings, V.J. et al. (2002) Smothering of estuarine sandflats by terrigenous clay: the role of wind-wave disturbance and bioturbation in site-dependent macrofaunal recovery. *Marine Ecology–Progress Series*, 234: 23–41.
- Périé, C., Ouimet, R. (2008) Organic carbon, organic matter and bulk density relationships in boreal forest soils. *Canadian Journal of Soil Science*, 88: 315–325.
- Petchy, F., Anderson, A., Hogg, A., Zondervan, A. (2008) The marine reservoir effect in the Southern Ocean: an evaluation of extant and new DR values and their application to archaeological chronologies. *Journal of the Royal Society of New Zealand*, 38(4): 243–262.
- Phillips, D.L., Inger, R., Bearhop, S., Jackson, A.L., Moore, J.W., Parnell, A.C., Semmens, B.X., Ward, E.J. (2014) Best practices for use of stable isotope mixing models in food-web studies. *Canadian Journal of Zoology*, 92: 823–835.

- Quinn, J., Phillips, C., (2016) Production forestry. In Jellyman, P.G., Davie, T.J.A., Pearson, C.P., Harding, J.S. (Eds) *Advances in New Zealand Freshwater Science. New Zealand Freshwater Sciences Society & New Zealand Hydrological Society.*
- Smith, J.N. (2001) Why should we believe ^{210}Pb sediment geochronologies? *Journal of Environmental Radioactivity*, 55: 121–123.
- Stevens, L., Robertson, B. (2010) Waimea Inlet: Vulnerability Assessment and Monitoring Recommendations. *Prepared for TDC*: 58.
- Stevens, L., Robertson, B. (2011) Waimea Inlet Historical Sediment Coring 2011. *Prepared for TDC*: 41.
- Stevens, L., Robertson, B. (2014) Waimea Inlet Broad-Scale Habitat Mapping. *Prepared for TDC*: 46.
- Stock, B.C., Jackson, A.L., Ward, E.J., Parnell, A.C., Phillips, D.L., Semmens, B.X. (2018) Analyzing mixing systems using a new generation of Bayesian tracer mixing models. *PeerJ*. 6, e5096; DOI 10.7717/peerj.5096.
- Thrush, S.F., Hewitt, J.E., Norkko, A., Nicholls, P.E., Funnell, G.A., Ellis, J.I. (2003a) Habitat change in estuaries: Predicting broadscale responses of intertidal macrofauna to sediment mud content. *Marine Ecology-Progress Series*, 263: 101–112.
- Thrush, S.F., Hewitt, J.E., Norkko, A., Cummings, V.J., Funnell, G.A. (2003b) Macrobenthic recovery processes following catastrophic sedimentation on estuarine sandflats. *Ecological Applications*, 13: 1433–1455.
- Thrush, S.F., Hewitt, J.E., Cummings, V., Ellis, J.I., Hatton, C., Lohrer, A., Norkko, A. (2004) Muddy waters: Elevating sediment input to coastal and estuarine habitats. *Frontiers in Ecology and the Environment*, 2: 299–306.
- Verburg, P. (2007) The need to correct for the Suess effect in the application of $\delta^{13}\text{C}$ in sediment of autotrophic Lake Tanganyika, as a productivity proxy in the Anthropocene. *Journal of Paleolimnology*, 37: 591–602.

Appendix A Study Proposal

24 May 2018

Environmental Information Manager
Tasman District Council
Private Bag 4,
Richmond 7050

Attention Rob Smith

Dear Rob

Sediment coring in the Waimea and Moutere Estuaries

Prior to his going on extended leave, I had discussions with Trevor James about the possibility of collecting two sediment cores, one each from the Waimea and Moutere estuaries. This is a continuation of the Waimea and Moutere River study which just been completed. Trevor was keen to get as much information as possible about contemporary sedimentation rates and sediment source contributions to these estuaries within a budget of \$45k. I believe he has talked with you about this. He suggested that I send this proposal to you for consideration.

We discussed various options and settled on taking a core from the Waimea Estuary at a site within the blue zone in the first photo. This is a site where TDC has a pin plate for estimating sediment accumulation and the sediment is mainly fine material and mud. The orange site has courser material and may not be suitable for lead-210 (^{210}Pb) dating.



Waimea Estuary sites.

Trevor was open to suggestions about the second site but would prefer to have a core taken in the Moutere Estuary within the green zone in the second photo. This zone contains deep soft sediment and should be ideal for his required purposes. The purple zone is within the intertidal flood area of the Moutere River and is likely to have large gravel members beneath the mud making coring difficult.



Moutere Estuary sites.

I have told Trevor that we could take the two cores, process them and provide a basic data report within his \$45k budget. This is based on the assumption that we use the same person to take the cores as we used in the Pelorus Sound study with Sean Handley, and that his charge hasn't changed substantially.

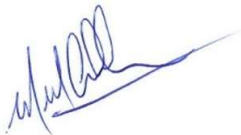
I estimate that we could take cores from the two sites (the blue zone in Waimea Estuary and the green zone in Moutere Estuary) and section them into between 12 and 15 slices each i.e., 24 to 30 samples total. The uncertainty in the number of slices is that we don't as yet have an updated price for the gamma analyses from ESR. I have heard that the cost has changed.

If we work on the basis of 12 slices per core, there is sufficient funds to do the core dating and CSSI modelling calculations and produce a basic data report with minimal interpretation. We would use the soil library from the previous river study for the modelling of the CSSI data. We need to do the ^{210}Pb dating to align the CSSI data with temporal changes and to enable us to apply the Suess correction to the CSSI and bulk carbon data.

Depending on the availability of the coring person, this work could be started this financial year and we could invoice for the whole project before the end of June, as required by Trevor.

If this is acceptable, NIWA would provide a standard IPENZ contract for this work, or we could use a TDC contract to undertake the work to a maximum cost of \$45,000 excluding GST. The expected output would be a basic data report with interpretation linked to the previous report on the Waimea and Moutere Rivers.

Best regards.



Max Gibbs
Water Quality Scientist

Appendix B ESR Core dating results



IANZ
ACCREDITED LABORATORY

Report number:	2019-312
Report date:	14/03/2019
Work Order Agreement number:	N/A

TEST REPORT

Client name:	NIWA	Order number:	TDC19201
Client's address:	PO Box 11115, Hamilton		
Samples submitted by:	Ron Ovenden	Date received:	31/01/2019
Samples analysed by:	Levi Bourke	Analyses started:	31/01/2019
Customer supplied description:	Sediment: 18 samples		
Sample received as:	Sediment, dry		
Analyses requested:	Pb-210, Cs-137, Ra-226, Ra-228		
Analytical methods:	Gamma spectrometry		

Concentration: If the measured value is above background at a level of confidence of 95%, then the concentration of the radionuclide is reported. The reported uncertainty is based on the combined standard uncertainty (u_c) multiplied by a coverage factor (k) = 2 (providing a level of confidence of 95%) as described by International Organization for Standardization, Guide to the expression of uncertainty in measurement, ISO, Geneva (1995).

Minimal Detectable Concentration: Reporting of a 'less than' result means that the measured value was consistent with a background measurement. The minimal detectable concentration with a level of confidence of 95% for both errors of the first and second kind is calculated according to ISO standard 11929 "Determination of the characteristic limits (decision threshold, detection limit and limits of confidence interval) for measurements of ionizing radiation – Fundamentals and application".

Traceability: Traceability to appropriate national or international standards is maintained. Details are available on request.

Scope of accreditation: All test results in this report are part of the laboratory's scope of accreditation unless marked otherwise.

Results

Sample number	Client code	Pb-210 (Bq/kg)		Cs-137 (Bq/kg)		Ra-226 (Bq/kg)		Ra-228 (Bq/kg)	
		Activity	Unc.	Activity	Unc.	Activity	Unc.	Activity	Unc.
2019-189	NIWA WA3 0-1	39.7	7.3	1.20	0.39	20.2	2.7	27.4	4.6
2019-190	NIWA WA3 4-5	40.7	7.5	1.21	0.42	19.7	2.7	26.2	4.6
2019-191	NIWA WA3 10-11	26.7	6.0	1.04	0.32	18.3	2.4	24.3	4.0
2019-192	NIWA WA3 14-15	27.9	6.0	1.27	0.32	17.4	2.3	21.6	3.5
2019-193	NIWA WA3 20-21	27.4	5.3	0.87	0.29	17.7	2.3	29	4.7
2019-194	NIWA WA3 24-25	26.3	5.1	1.05	0.35	17.1	2.3	30.3	4.9
2019-195	NIWA WA3 29-30	23.7	4.7	0.58	0.24	18.6	2.4	28.4	4.6
2019-196	NIWA WA3 34-35	21.3	4.4	< 0.61	N/A	15.8	2.1	27.0	4.4
2019-197	NIWA WA3 39-40	15.1	4.3	< 0.50	N/A	15.5	2.0	25.2	3.9

Sample number	Client code	Pb-210 (Bq/kg)		Cs-137 (Bq/kg)		Ra-226 (Bq/kg)		Ra-228 (Bq/kg)	
		Activity	Unc.	Activity	Unc.	Activity	Unc.	Activity	Unc.
2019-198	NIWA Mo4 0-1	26.4	4.7	< 0.53	N/A	18.7	2.4	24.0	3.9
2019-199	NIWA Mo4 4-5	23.2	6.9	< 0.40	N/A	19.5	2.5	23.4	3.7
2019-200	NIWA Mo4 7-8	25.8	4.9	< 0.51	N/A	19.3	2.5	25.0	4.1
2019-201	NIWA Mo4 10-11	21.2	4.2	< 0.66	N/A	20.2	2.6	29.8	4.8
2019-202	NIWA Mo4 14-15	18.9	4.6	< 0.53	N/A	21.0	2.7	29.4	4.5
2019-203	NIWA Mo4 17-18	21.2	4.2	< 0.54	N/A	22.3	2.8	33.5	5.2
2019-204	NIWA Mo4 20-21	19.4	5.0	< 0.49	N/A	20.4	2.6	27.3	4.2
2019-205	NIWA Mo4 24-25	22.7	4.7	< 0.66	N/A	20.7	2.7	33.1	5.3
2019-206	NIWA Mo4 29-30	22.3	5.2	< 0.48	N/A	19.5	2.5	27.9	4.3

Report date: 14 March 2019 Report No: 2019-312

Page 2/3

ERL/FORM/6/004 V2

Additional Information

Results relate only to the samples as received.

Validity of results is based on true and correct customer supplied description.

This report, or any copy of it, is only valid if it is complete.



Dr Michael Lechermann, Radiation Physicist

Date: 14/03/2019

Appendix C Isotopic data

Sediment core WA3

Seuss corrected Fatty Acid isotopic signatures for the WA3 sediment core slices

Depth (cm)	year	$\delta^{13}\text{C}$	c14:0	C16:0	c18:0	c18:1w9c	18:2w6c/6	c20:0	c22:0	c24:0
1.5	2016	-24.53	-30.79	-29.63	-29.59	-28.62	-24.97	-31.29	-30.16	-30.48
5.5	2010	-24.55	-29.57	-29.72	-29.85	-29.28	-27.93	-31.22	-30.48	-30.44
7.5	2008	-24.57	-28.48	-27.58	-29.38	-27.09	-27.90	-31.38	-30.04	-30.07
9.5	2005	-24.27	-30.32	-30.92	-29.40	-26.55	-24.58	-31.24	-29.91	-29.71
11.5	2002	-24.12	-30.32	-31.49	-28.93	-31.67	-26.58	-30.36	-29.20	-29.37
13.5	1999	-24.07	-30.61	-31.33	-28.81	-27.14	-27.29	-30.22	-28.88	-29.14
16.5	1995	-23.68	-29.99	-30.51	-29.41	-25.90	-24.72	-30.45	-29.24	-29.18
18.5	1992	-23.42	-29.70	-29.16	-28.08	-25.46	-24.92	-28.38	-28.81	-28.89
21.5	1988	-23.43	-30.37	-30.63	-28.81	-25.91	-26.78	-29.64	-28.27	-28.55
23.5	1985	-23.17	-30.38	-29.96	-29.13	-26.10	-27.14	-29.76	-28.56	-28.29
25.5	1983	-22.93	-30.40	-30.19	-28.66	-25.18	-25.33	-29.70	-28.54	-28.24
27.5	1980	-22.81	-29.60	-28.92	-28.13	-25.23	-24.46	-29.65	-28.45	-28.09
30.5	1976	-22.64	-28.90	-29.14	-27.50	-24.29	-23.44	-29.13	-28.04	-27.53
32.5	1973	-22.46	-28.73	-28.05	-27.83	-24.48	-25.46	-29.07	-27.72	-27.24
33.5	1971	-22.54	-27.93	-29.79	-28.51	-25.19	-27.84	-28.63	-27.20	-27.02

Soil sources

Code	%C	d13C	c14:0	c16:0	c18:0	c18:1w9c	c18:2w6c/6t	c20:0	c22:0	c24:0
BankAg	1.15	-27.44	-28.97	-27.79	-30.92	-29.50	-28.71	-34.16	-32.77	-33.65
G_&_B	3.15	-26.34	-32.68	-30.40	-27.54	-30.85	-29.53	-32.41	-32.11	-32.91
Native	9.05	-28.30	-34.87	-31.31	-31.16	-30.75	-30.06	-33.02	-33.33	-33.69
Pasture	8.96	-28.38	-32.54	-30.15	-30.95	-30.57	-30.70	-34.19	-34.10	-34.38
PineH	4.44	-26.87	-30.93	-27.71	-27.28	-28.48	-29.35	-30.74	-30.66	-30.85
PineM	4.39	-28.27	-37.35	-32.50	-29.94	-28.85	-31.99	-30.88	-30.59	-31.60
PineR	2.74	-27.99	-32.63	-31.01	-28.35	-31.97	-27.64	-27.88	-26.94	-27.30
Subsoil	1.03	-27.25	-31.27	-29.12	-27.70	-28.52	-27.69	-28.88	-28.79	-29.01

Appendix D Floods in the Tasman District

The floods in the Tasman and Nelson Districts between 1970 and 2016 have been extracted from the NIWA “NZ Historic Weather Events Catalog” (available at <https://hwe.niwa.co.nz/>) and are presented below:

March 2016 New Zealand Storm

A period of extreme weather affected many areas of New Zealand on 24 March. There was flooding on the West Coast of the South Island, and around the Nelson area. Strong winds affected areas around Auckland and Northland.

June 2015 New Zealand Storm

A period of extreme weather affected many areas of New Zealand during the period 18-23 June. There was heavy snow in the South Island followed by severe frosts, and severe flooding in western areas of the South and North Islands.

June 2015 Otago Flood

A low pressure system to the southeast of the South Island brought heavy rainfall to coastal Otago on 3 June 2015. Every coastal catchment from Oamaru south to Balclutha experienced some degree of flooding during this event.

April 2014 New Zealand Storm

Ex-tropical cyclone Ita lay to the west of the North Island bringing heavy rain and strong winds. It moved southwards during the period 17-19 April. The very strong winds caused lots of damage, and brought down power lines, cutting the power supply to thousands of homes. Heavy rain also caused flooding. The worst affected area was the West Coast of the South Island.

April 2013 Upper North Island and Nelson Storm

Clashes of cold south-easterly and warm northerly airmasses, from a large and complex low pressure system in the Tasman Sea, brought wet and unsettled weather to many areas of New Zealand. The worst weather during this period were very heavy rainfalls in the western Bay of Plenty on the 20th and in the Nelson region on the 21st.

May 2010 Tasman-Nelson Flooding

There were thunderstorms across New Zealand and a tornado in Taranaki which caused some damage. Tasman-Nelson was hit with heavy rain which caused flooding in the Tapawera area. 22 households were evacuated.

November 2008 Upper South Island Flooding

Heavy rain brought flooding to the Nelson-Tasman region, Marlborough and the West Coast. There was also heavy rain in parts of the North Island, mainly Taranaki, and high winds hit various places across the country.

August 2008 Central New Zealand Heavy Rain

The third storm of three in a one-week period. Heavy rain and thunderstorms throughout central New Zealand caused further damage, particularly in Wellington where landslips caused evacuations.

July 2008 Nelson Flooding

Heavy rain caused flooding in Nelson on the morning of the 11th and also on lower North Island roads overnight and on the 12th.

April 2008 North Island and Nelson Storm

Many parts of the North Island, plus Tasman-Nelson, experienced electrical storms, heavy rain, flooding, slips and high winds. The 'Mangatepopo Tragedy' occurred, in which seven people drowned and one person was injured in Tongariro National Park. During a hunt near Dargaville, lightning killed one man and injured five others.

May 2007 Tasman-Nelson and Taranaki Flooding

Flash floods hit New Plymouth and Nelson on the 23rd.

January 2005 New Zealand Flooding

Heavy rain caused flooding in Manawatu-Wanganui, Wellington, Tasman-Nelson and Otago. The hardest area hit as Wellington where hundreds of people had to be evacuated.

January-February 2004 New Zealand Flooding

Heavy rain was experienced in Northland, Auckland, Waikato, Taranaki, Wanganui, Wellington, Marlborough, Nelson and the West Coast, bringing flooding to some areas. In Taranaki, a man drowned in the flooded Waiwhakaiho River. A man also drowned in Nelson when his car plunged into a swollen river. Homes were flooded in Wanaka.

January 2002 North Island and Upper South Island Thunderstorms

Thunderstorms brought lightning, heavy rain and flooding to many parts of the North Island and upper South Island. Wellington and Hawke's Bay were the worst affected regions, with extreme rainfalls causing flooding of properties and streets. A person in Auckland was treated for an eye injury caused by a sewage overflow.

October 1998 Western New Zealand Flooding

This storm followed the 18-21 October storm and affected the same areas. The ground was still sodden and prone to flooding resulting in hundreds of evacuations and Civil Defence emergencies along the west coast of New Zealand. There was one casualty due to the event in the Wellington region.

October 1998 North Island and Upper South Island Flooding

Heavy rain brought flooding and slips to parts of the North Island and upper South Island. Rainfall in Taranaki was extreme, and extensive damage was done to roads.

July 1998 New Zealand Flooding

Heavy rain fell in Waikato, Bay of Plenty, Wellington, Marlborough, Tasman-Nelson and the West Coast, bringing flooding and slips to some places. Te Kuiti recorded rainfall with a return period of over 100 years.

June-July 1997 Upper North and South Island Flooding

Heavy rain brought flooding to Northland, Waikato, Bay of Plenty and Hawke's Bay in the North Island, and high winds were also experienced. Heavy rain and flooding occurred in Marlborough, Nelson and the West Coast in the South Island. Parts of Northland experienced extreme rainfall, and a man was injured when a car hit him as he stood in flood waters. One person was killed when a car hit a fallen tree.

August 1990 Tasman-Nelson Flooding and the Taranaki Tornado

Severe damage to homes and businesses occurred when a tornado hit Bell Block and Inglewood on the 12th of August 1990. Tasman-Nelson experienced heavy rain causing extensive flooding in the Motueka area and resulting in millions of dollars' worth of damage. Marlborough also experienced some flooding.

April 1990 Tasman-Nelson Storm

An electrical storm and heavy rain hit Nelson on the 27th of April causing power failures and road closures.

March 1988 North Island Ex-tropical Cyclone Bola

Ex-tropical Cyclone Bola struck most regions of the North Island, in particular Taranaki, Hawke's Bay, Gisborne and Northland, bringing widespread damage with combinations of heavy rain, flooding, high winds and heavy seas. Two people were drowned in Northland, three in Gisborne and two in Hawke's Bay. Three people were injured by high winds in Taranaki. The tail end of the cyclone later struck Tasman-Nelson.

January 1986 Nelson Flooding

Heavy rain brought severe flooding and slips to the Nelson area. A Civil Defence Emergency was declared for the region, and properties and roads were damaged. A boy was drowned in a Nelson stream.

October 1983 Marlborough and Tasman-Nelson Flooding

Severe flooding and slips closed roads and Civil Defence emergencies were declared for both Tasman-Nelson and Marlborough.

July 1983 Upper South Island Flooding

Heavy rain caused severe flooding especially in Marlborough and Golden Bay.

April 1976 Northland and Tasman-Nelson Winds and Flooding

High winds were experienced in Northland and Tasman-Nelson. Extreme rainfall brought flooding to the northern Tasman-Nelson area, and one woman was drowned.

April 1975 Tasman-Nelson and Marlborough Flooding

A weather bomb caused flooding in Marlborough.

March 1975 New Zealand Ex-tropical Cyclone Alison

Ex-tropical Cyclone Alison caused high winds, heavy rain, flooding, slips and high seas around many parts of New Zealand. Much damage was done to roads, rail and both public and private property. A girl died in the Waikato after she touched a felled electric wire. A car accident on a flooded road in Canterbury saw one woman killed and a girl injured. Some people were also injured when a car fell into a road subsidence in Christchurch.

March 1975 Tasman-Nelson Flooding

Heavy rain caused flooding in the Tasman-Nelson region. The Golden Bay area was hit the hardest.

August 1970 Upper South Island Flooding

Heavy rain, flooding, slips and high winds occurred in parts of the upper South Island. Roads and properties were affected. Flooding was severe in the Nelson area, and two women were killed, one by a flooded stream and one by a landslide.